

Concentration Profiles in Photo-Curing Porous Coatings

Hirokazu Yoshihara^{1,2} and Masato Yamamura²

¹*Dai Nippon Printing Co., Ltd.,*

²*Department of Applied Chemistry, Kyushu Institute of Technology.*

Corresponding author: yamamura@che.kyutech.ac.jp

ISCST-20180917PM-B-DF2

Presented at the 19th International Coating Science and Technology Symposium, September 16-19, 2018, Long Beach, CA, USA[†].

Keywords: drying, UV curing, polymerization, diffusion, Raman spectroscopy

Introduction

Solvent/monomer/initiator ternary solution films exhibit a polymerization reaction upon irradiation of ultra-violet (UV) light. Immiscibility between the polymer and solvent leads to show a phase separation between polymer-rich and solvent-rich phases. However, it is challenging to fabricate uniform phase structures because of complicated reaction-diffusion coupling. Despite practical utilities of the photo-induced phase separation to create nanoscale pores inside the film^[1], little attention has been paid to evolutions of concentration profiles before/after the photo irradiation. In this study, we utilize confocal Raman spectroscopy^[2] to directly determine local polymer concentrations in photo-polymerized films. In order to gain high spatial resolutions, we developed a novel technique to replace residual solvent with monomer, minimize reflective index differences, and avoid strong light scattering from phase-separated microstructures.

Experimental

Material and conditions

We used methyl-isobutyl ketone (MIBK, Wako) as solvent, multifunctional polyester acrylate (M9050, Toagosei Mw:1000-1500) as photo-reactive monomer, and 1,3 α -alkyl amino phenone (IRUGACURE379EG, BASF Mw:380.52) as photo-initiator. The initial solvent-to-nonvolatile mass ratio was 6:4 (wt/wt) and monomer-to-initiator ratio was fixed at 95:5 (wt/wt). Experimental conditions are summarized in Table 1.

Table 1 Experimental conditions

Temperature	25 °C
Wet thickness	100 μ m
Drying after curing	Under free convection
UV wavelength	365 \pm 2nm
UV intensity	0 ~7500 mJ/cm ²

Experimental method

The solution was dropped on a glass plate (Fig. 1a), and sandwiched between two glass plates of a uniform clearance of 100 μ m predetermined by a feeler gauge. The UV light with a wavelength of 365 \pm 2 nm was irradiated from the top to induce the radical polymerization reactions (Fig.1b). SEM images of the cured samples indicated evolutions of phase-separated porous structures (not shown). The solvent evaporation during the photo-curing was negligible slow because of the confined geometry. After a certain curing of less than 10 s, the film was peeled off from the bottom-side glass plate (Fig.1c). 10 ml liquid monomer was dropped onto the film to replace the solvent in pores with the monomer (Fig.1d). Subsequently, the sample was set on the hot plate to evaporate solvent at 45 °C for 15 minutes (Fig.1e). Finally, the dried film was re-sandwiched between two glass plates (Fig.1f).

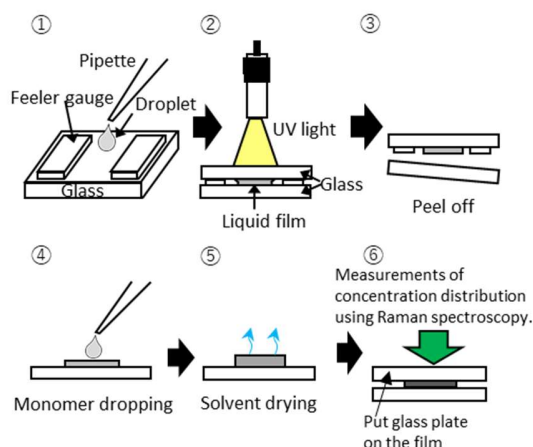


Fig.1 Experimental method

[†] Unpublished. ISCST shall not be responsible for statements or opinions contained in papers or printed in its publications.

Raman spectroscopy

We used confocal Raman spectroscopy (DXR2 Raman Microscope, Thermo-Scientific) to evaluate composition distribution of each chemical component inside the UV-cured films. The excitation laser light of $532\pm 2\text{nm}$ in wavelength was irradiated through an objective lens onto the sample. The Raman signal was collected by an objective lens and sent to a spectrometer through a Rayleigh-light-cut filter as shown in Fig. 2.

The focus of the laser was scanned in the depth direction with an accuracy of $0.2\ \mu\text{m}$. The position of the glass-film interface was determined from the absolute mechanical position in the z-axis direction and the thickness of the glass plate.

In order to determine local concentrations, we used calibration curves of Raman peak intensities taken from the data of solutions with known concentrations [2]. The typical example of the Raman spectrum of the ternary solution is shown in Fig.3. Three distinct peaks of $600\ \text{cm}^{-1}$, $1640\ \text{cm}^{-1}$, and $1600\ \text{cm}^{-1}$ were associated with specific chemical bonds in solvent, monomer, and initiator, respectively, and used for the composition analysis.

Fig.4 shows an example of the calibration curve: the initiator-to-solvent peak height ratios plotted against the mass ratios, where W_s , W_m , and W_i represent the mass fraction of solvent, monomer, and initiator in a ternary solution, and I_s and I_i represent the peak intensities at $600\ \text{cm}^{-1}$ and $1600\ \text{cm}^{-1}$, respectively. The good linear relationship between the mass-intensity ratios enables us to calculate the composition from the measured intensity.

Monomer conversion

The monomer conversion was defined as the difference in monomer contents before and after the photocuring divided by the initial monomer content. To quantify the variations in monomer content, we focused on a Raman peak at $2960\ \text{cm}^{-1}$, which is attributed to C-H bond included in MIBK (I_{CH_s}), M9050 (I_{CH_m}), and polymer (I_{CH_p}). We assumed that the peak height is given by a sum of those for each component. Indeed, preliminary Raman measurements for solvent-monomer binary solutions indicate that the peak height at $2960\ \text{cm}^{-1}$ is proportional to I_s and I_m , respectively. The conversion (P) is calculated from equation (1), where the constants α , β , and γ are determined from Raman spectra for each pure component.

$$P(\equiv 1 - \frac{I_m}{I_{m0}}) = 1 - \frac{1}{\frac{1}{\gamma}(I_{\text{CH}}/I_m - \alpha I_s/I_m - \beta) + 1} \quad - \quad (1)$$

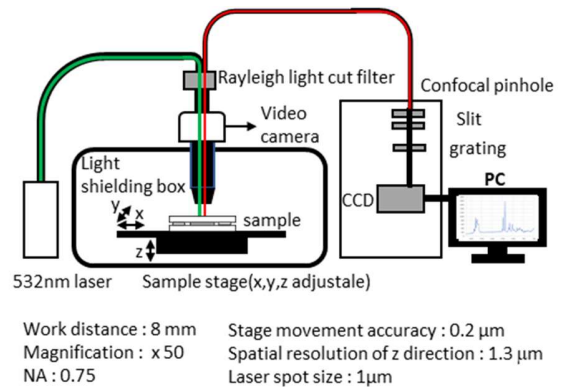


Fig.2 Set up of the confocal Raman spectroscopy

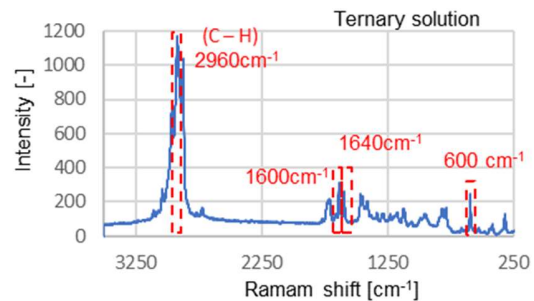


Fig.3 Raman spectrum of ternary solution at the mass ratio of solvent:monomer:initiator = 60 : 38 : 2 (wt/wt)

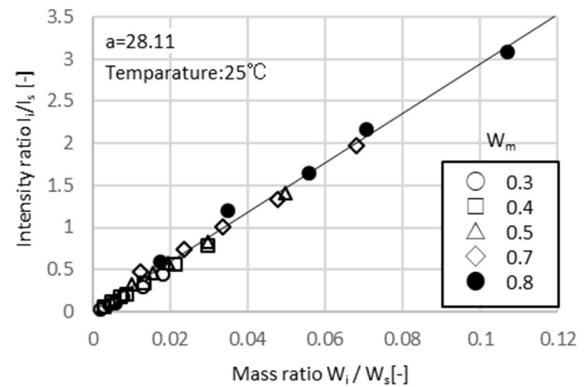


Fig.4 Caribration curve of intensity ratio I_i/I_s with respect to the mass ratio W_i/W_s

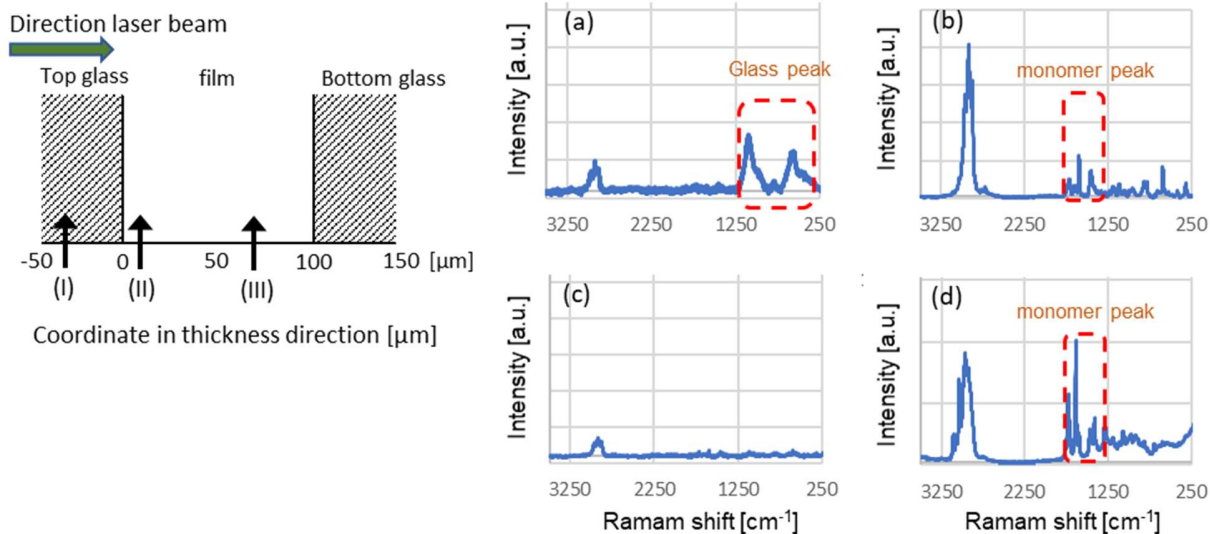


Fig.5 Raman spectra at (a) position I, (b) position II, (c) position III before the solvent replacement, and (d) position III after the replacement

Results and Discussion

Raman spectroscopy at different depth positions

Fig.5 shows the typical examples of Raman spectra at different depths before and after the solvent replacement. The peaks associated with Si-O-Si bonds in glass substrate were observed at outer regions of the sample (Fig. 5a). Weak peaks of the monomer appeared in the vicinity of sample-glass interface (Fig.5b), but diminished as the focus moved deeper in the coating (Fig.5c). This is possibly because the refractive index of the polymer ($n = 1.520$) was too high compared to that of the solvent ($n = 1.396$), leading to a light scattering that could reduce the Raman signals.

On the other hand, replacing the solvent with the monomer allowed us to obtain distinct peaks associating with the monomer at the same position (Fig. 5d). The supplemental measurements of the refractive index of the monomer showed $n = 1.499$, which is closer to that of the polymer. These facts imply that our procedure of solvent replacement in porous films enables to prevent light scattering at interfaces of the polymer domains.

Polymer concentration distributions at different UV intensities

To examine effects of UV irradiation conditions on concentration profiles, we measured the polymer concentration distributions inside porous films at different UV light intensities. As shown in Fig. 6, the polymer concentration monotonically increases with increasing light intensity. The local polymer concentration at the bottom side is lower than the top at any UV intensities. At high intensities, the polymer concentrations are uniform in the vicinity of the top surface, and decrease as the UV light penetrates deeper in the coating.

It is worth noting that the difference in polymer concentration at the top and bottom surfaces first increases and then decreases as increasing UV light intensity. Although the physical mechanism is under investigation, our previous study^[3] imply that the UV irradiation promotes the solvent diffusion

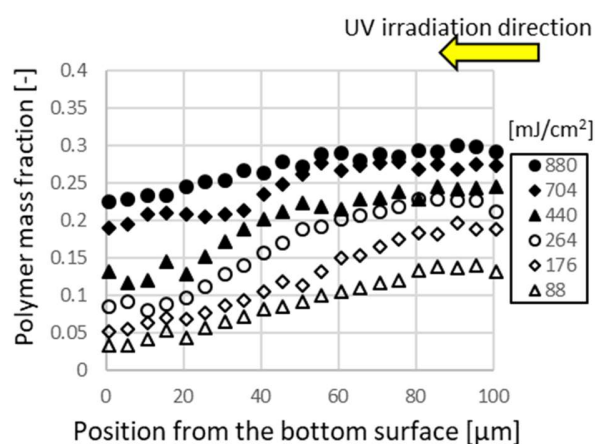


Fig.6 Polymer concentration distributions inside films at different UV light intensities

from the top toward the bottom at a certain range of UV intensities. The reaction-diffusion coupling possibly reduces the polymer concentration at the bottom, and tends to increase the concentration gradient.

.

References

- [1] H. Nakanishi, T Norisuke, Q.T.Miyata, J. Phys Chem Lett. 2013, 4, 3978-3982.
- [2] P. Scharfer, W. Schabel, M. Kind, J. Membrane Science 303 (2007) 37-42.
- [3] H. Yoshihara, M. Yamamura, Proceeding of the 17th European Coating Symposium, Switzerland, 2017(Nov8-10), 140-142.